2012

Efficient and Robust Training Methodology for Inverse Building Modeling and Its Application to a Multi-zone Case Study

Jie Cai
cai40@purdue.edu

James E. Braun

EFFICIENT AND ROBUST TRAINING METHODOLOGY FOR INVERSE BUILDING MODELING AND ITS APPLICATION TO A MULTI-ZONE CASE STUDY

Jie Cai[1]* and James E. Braun[2]

[1]Ray W. Herrick Laboratory, Purdue University, US
cai40@purdue.edu

[2] Ray W. Herrick Laboratory, Purdue University, US
jbraun@purdue.edu

* Corresponding Author

ABSTRACT

This paper presents an efficient and robust parameter training methodology, based on a previous approach for inverse building modeling that utilizes a simplified state-space approach. One new element of this training methodology is that some seasonal effects, such as variation of window transmittance at different times of the year, are taken into consideration and captured during the training process. In addition, a mixed-mode training approach is developed that allows the use of a combination of data obtained when cooling or heating is occurring with the zone temperature under control at setpoint and when the zone temperature is floating during periods of no load. To obtain a "nearly" global optimal model, a multi-start search method was found to be robust and provide good computational efficiency and accurate results. The training methodology is implemented to model three zones of Building 101 at the Navy Ship Yard in Philadelphia, Pennsylvania.

1. INTRODUCTION

Forward building models, such as those employed in EnergyPlus (2011) and TRNSYS (2010), require many geometrical and physical parameters and are appropriate for system design but are not ideal for online applications, such as real-time control or fault identification. Inverse building models typically utilize simplified modeling approaches with lumped parameters where the parameters are learned using data collected from a specific building site. When properly trained, these types of models can provide more accurate and computational efficient load predictions for a specific building and are more appropriate for the operational phase of the building cycle. In addition to real-time control and fault identification, these types of models can be used in analyzing retrofit opportunities.

2. MODEL STRUCTURE AND UNKNOWN PARAMETERS

2.1 Model Structure

Previous studies (Chaturvedi, 2000) have shown that a two-node representation of a single wall provides a reasonably accurate approximation of the actual wall. Based on this starting point, a simplified structure of a zone can be proposed using two nodes to represent each wall. A simplified whole building model that was developed by Chaturvedi and Braun (2002) is shown in Figure 1. In this representation, all of exterior walls are combined into a single exterior wall with an external boundary condition that includes the total incident radiation on all wall surfaces. Solar radiation that is transmitted through windows is assumed to be absorbed equally on two sides of an interior wall presentation. The interior wall also captures the effects of floors between stories of a multi-story building. An additional ground element is included to capture ground coupling dynamics. Internal radiative gains are assumed to be distributed with an even flux to walls and ceiling, whereas convective internal gains go directly to the zone air. A pure resistance is included to capture the effects of heat transfer across low-mass elements, such as windows or due to infiltration.

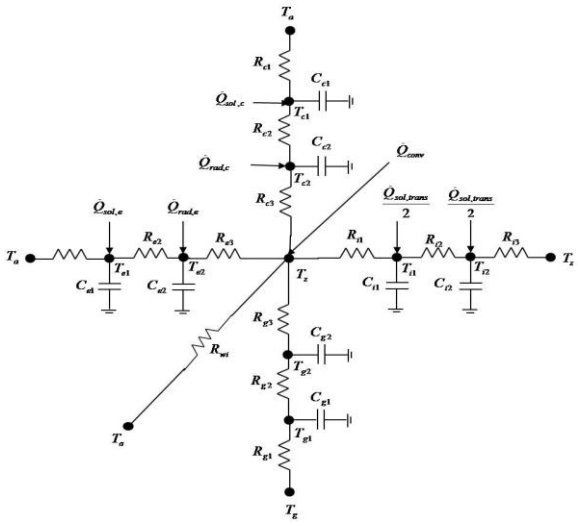

Figure 1: Thermal network for a single zone building model.

Applying an energy balance to each node in the network, a state-space representation can be established for this simplified model structure:

$$\frac{d\mathbf{x}_b}{dt} = \mathbf{A}_b\mathbf{x}_b + \mathbf{B}_b\mathbf{u}_b \tag{1}$$

$$\mathbf{Y}_b = \mathbf{C}_b\mathbf{x}_b + \mathbf{D}_b\mathbf{u}_b \tag{2}$$

where $\mathbf{Y}_b$ is the output, which can be either cooling load (zone air temperature is input) or zone air temperature (cooling load is input).

For the case of cooling load being the output, the state and input vectors are:

$$\mathbf{x}_b^T = [\ T_{c1}\ T_{c2}\ T_{e1}\ T_{e2}\ T_{g1}\ T_{g2}\ T_{i1}\ T_{i2}\ ]$$

$$\mathbf{u}_b^T = [\ T_z\ T_a\ T_g\ \dot{Q}_{sol,c}\ \dot{Q}_{sol,e}\ \dot{Q}_{rad,c}\ \dot{Q}_{rad,e}\ \dot{Q}_{sol,trans}\ \dot{Q}_{conv}\ ]$$

For the case of zone air temperature being the output, the state and input vectors are:

$$\mathbf{x}_b^T = [\ T_{c1}\ T_{c2}\ T_{e1}\ T_{e2}\ T_{g1}\ T_{g2}\ T_{i1}\ T_{i2}\ T_z\ ]$$

$$\mathbf{u}_b^T = [\ \dot{Q}_b\ T_a\ T_g\ \dot{Q}_{sol,c}\ \dot{Q}_{sol,e}\ \dot{Q}_{rad,c}\ \dot{Q}_{rad,e}\ \dot{Q}_{sol,trans}\ \dot{Q}_{conv}\ ]$$

2.2 Unknown Parameters

The set of parameters to be estimated can be denoted as:

$$\theta = \{\theta_1, \theta_2\}$$

where

$$\theta_1 = [C_{e1}\ C_{i1}\ C_{c1}\ C_{g1}\ R_{e1}\ R_{e2}\ R_{i1}\ R_{i2}\ R_{c1}\ R_{c2}\ R_{g1}\ R_{g1}\ R_{g2}\ C_{e2}\ C_{i2}\ C_{c2}\ C_{g2}\ R_{e3}\ R_{i3}\ R_{c3}\ R_{g3}\ ]$$

$$\theta_2 = [Q_{\text{int,gain}}\ R_{\text{conv}}\ a_{\text{trans}}\ b_{\text{trans}}]$$

The first group θ_1 consists of all resistances of both the walls and the window, and capacitance values of the walls in the thermal network in Figure 1. The resistances and capacitances determine the entries within the matrices A_b, B_b, C_b, and D_b of Equations (1) and (2). The second group θ_2 contains parameters that are used for all other purposes. The first two parameters in the 2nd group are used for the rate of internal gains ($Q_{\text{int,gain}}$) during the occupied period and the ratio of the convective component (R_{conv}) to the total internal gains. When the model is trained using data

generated from simulation tools like TRNSYS, the internal gains can be exported as input for the model and these two parameters are just place keepers. But when using actual field data for training, it is not possible to measure the actual internal gains. In this case, the internal gains and their effect should be captured in the training and the quantities are represented by these two parameters. In our case, an assumption was made for this study that during the unoccupied period, the internal gains are zero while in the occupied period they are a constant gain of $Q_{\text{int,gain}}$. This internal gain splits between convective and radiative components at a fixed ratio, which is denoted by $R_{\text{conv}}/(1-R_{\text{conv}})$. The other two parameters (a_{trans}, b_{trans}) are used in modeling the variation of transmittance versus the incident solar angle for the window. The details are illustrated in the following section.

2.3 Transmittance variation

Window transmittance can be classified into beam and diffuse radiation transmittance (Arastehet al., 2009). Beam transmittance varies with incidence angle while diffuse transmittance is constant. Based on typical trends for window transmittance with incidence angle, the following correlations were developed:

$$T_{beam} = T * F = T * (1 - a_{trans}\alpha^{n})$$
$$T_{diff} = T * b_{trans}$$

where T_{beam} and T_{diff} represent beam and diffusive transmittance, α is solar incidence angle and n is an integer power assumed to be one in this study. a_{trans} and b_{trans} are correlation coefficients, which are also parameters to be estimated. T is the normal transmittance, which is taken as the solar heat gain coefficient value (SHGC) associated with each window model for simplicity. The estimation of a_{trans} and b_{trans} is embedded in the whole training process and some results of tested cases are shown and explained by Cai and Braun (2012). It was found that implementing this transmittance correlation leads to a more accurate model for annual simulations with the RMS error cut almost by half within a specific testing period compared to the model obtained without transmittance variation.

3. PARAMETER ESTIMATION

3.1 Problem Formulation

For a fixed set of parameter values (θ is fixed), the methodology of Seem et al. (1989) can be used to solve the state-space representation, and to predict cooling load or zone air temperature of the building as a transfer function of the input and state variables. In this study, the time step of the transfer function is assumed to be one hour. The solution for the output is given as:

$$y_{b,k} = \left(\sum_{j=0}^{8} \mathbf{S}_{b,j}\mathbf{u}_{b,k-j}\right) - \left(\sum_{j=1}^{8} ue_{b,j}\, y_{b,k-j}\right)$$

where

$y_{b,k}$ = output (either $\dot{Q}_{b,k}$ or $T_{b,k}$) at time k;

$\mathbf{S}_{b,j}$ = series of row vectors containing transfer function coefficients for the input matrix in the building state-space representation;

$e_{b,j}$ = scalar transfer function coefficients for past histories of the output.

The calculation of the coefficients $\mathbf{S}_{b,j}$ and $e_{b,j}$ from matrices $\mathbf{A}_b$, $\mathbf{B}_b$, $\mathbf{C}_b$ and $\mathbf{D}_b$ is outlined by Seem et al. (1989).

For a specific parameter value set, the performance of the model can be evaluated in terms of how well the output (or prediction) matches the actual data (baseline). A commonly used criterion for the deviation of prediction from baseline is least-square error:

$$J_{b,\theta} = \sqrt{\frac{\sum_{k=1}^{Ntrain} (y_{b,k} - y_{actual,k})^{2}}{Ntrain - 1}}$$

where

$J_{b,\theta}$ = optimization regression cost function at point θ;

$y_{actual,k}$ = baseline output at time step k;

$Ntrain$ = training duration in hours.

So the formulation of our parameter estimation problem can be written as:

$$\theta^* = \arg\min_{\theta \in \Omega} \left(J_{b,\theta} \right)$$

where Ω is the search region for the parameter values in the estimation process. This search region is determined according to the information available about the zone. This information can be obtained via several means, such as by requesting a survey from the building administrator or by looking at the blueprint of the building. Generally speaking, the less information we have about the building, the bigger the search region is for the optimization. When the search region is big, the estimation process could more easily converge to a local optimum. So some preprocessing is necessary in obtaining a good initial guess to improve the chances of obtaining a global optimal point.

3.2 Global-Local Search

In the previous work by Chaturvedi and Braun (2002), a global-local search scheme was adopted (see Figure 2) for parameter estimation. A global phase was applied in order to obtain a global optimal estimation of the parameter values, and a systematic search algorithm developed by Aird and Rice (1977) was implemented. It is similar to grid search but more generalized in the sense that any number of points can be generated in the search space with the property that the dispersion of the generated set is minimized. At each of these generated points, the least-square error is evaluated and the point with a smallest least square error is chosen as an initial guess for the local search.

In the local search phase, the Levenburg-Marquardt algorithm (Madsen et al., 2004) is used. This LM algorithm interpolates between the Gauss-Newton and the gradient descent method but it shows more robustness than the Gauss-Newton algorithm.

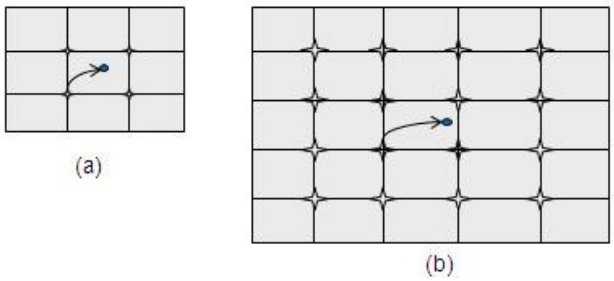

Figure 2: (a) Small search region. (b) Large search region, in which the number of point evaluations is increased to maintain the same level of gridding.

3.3 Multi-Start Search

When very limited information about a building is available, the search region becomes large and it is not feasible to use the global-local search scheme. In this situation, a multi-start search scheme would be more suitable since this type of method is often applied for large-scale estimation problems (Aster et al., 2005).

In a multi-start search process, several points are generated pseudo-randomly as initial guesses for regression and the regression is performed for each point. The solution with the smallest least square error is chosen to be the final parameter values.

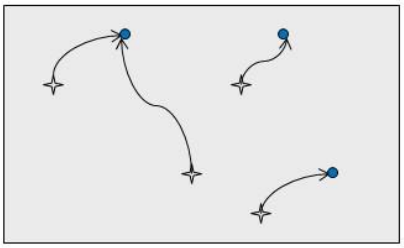

Figure 3: Multi-start search scheme.

Some comparisons have been carried out in terms of performances for these two search algorithms and results are given by Cai and Braun (2012). In the comparison, multi-start search method shows more robustness and efficiency when parameter search region is large.

3.4 Mixed Training Mode

There are two modes in which models can be trained. In one mode, the training process takes zone air temperature as input and predicts cooling load, while in the other mode, the input and output are switched. In a real operational phase, the zone air temperature may be floating sometimes when the cooling equipment is off, such as during the unoccupied period and at other times it may be under control (e.g., positive cooling load in the occupied period). The fraction of the time that there is a cooling load changes with seasons and control strategies. When the zone temperature is under control, there are no dynamics in the zone temperature output so it is better to train the model using cooling load as the output. Conversely, when the cooling is off and the temperature is floating, temperature is the preferred output for training. Based on this analysis, a mixed training mode is proposed whereby the training mode switches from cooling or zone temperature as an output according to which output has better dynamics. Figure 4 shows the mechanism of this training process.

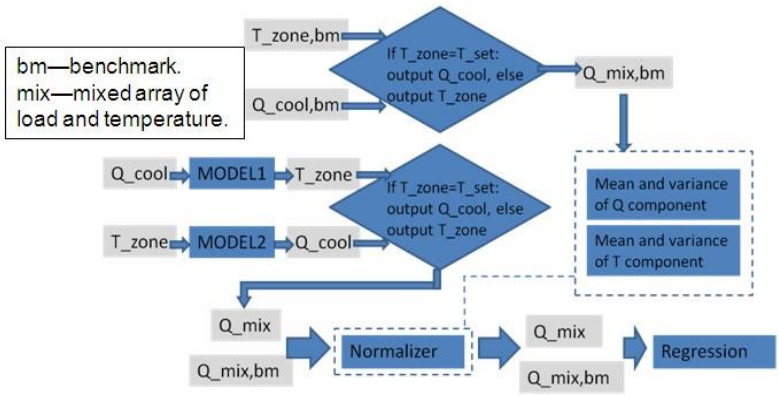

Figure 4: Mechanism of mixed training process.

Some testing results are listed by Cai and Braun (2012). The mixed training provides better overall results compared to a single training mode, especially when there is a relatively equal mix of floating and controlled zone temperatures in the training set.

4. NAVY SHIPYARD BUILDING 101 CASE STUDY

The primary focus of the current paper is to adapt the inverse modeling techniques described above to a multi-zone case study that is based on the Navy Shipyard Building 101 located in Philadelphia, PA. Training data for this paper was generated using a TRNSYS model developed for a section of this building. In the future, on-site data will be used for training the inverse model.

4.1 Multi-Zone Description

Building 101 is a three-floor building divided into three main sections: northwing, southwing and middle section. There are nine zones in the northwing that are served by one air-handling unit (AHU). Our case study is focused on three zones that are on the second floor in the northwing, which are labeled as Z8, Z2 and Z3 in the floor layout in Figure 5.

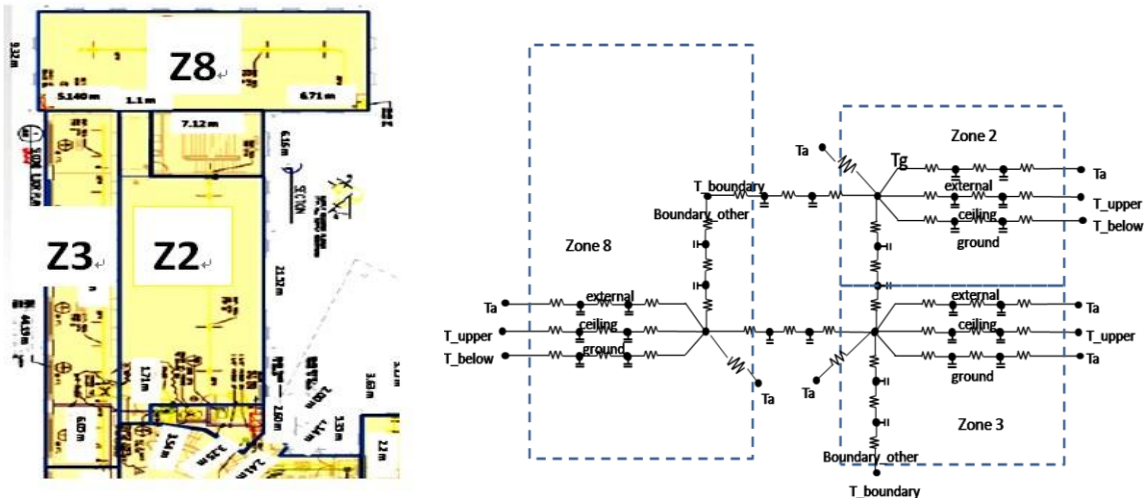

Figure 5: Floor layout and thermal network for three zones.

Figure 5 also shows the thermal network of the three zones that are to be studied. This thermal network is built up based on the single-zone thermal network shown in Figure 1. But there are several modifications that are made to each of the zones. For all zones in this specific case study, there are no internal walls so the internal wall branches are taken out. But each zone has additional coupling wall(s) and boundary walls so related branches are inserted. The transmitted solar radiation is applied to the floor instead of the internal wall. In the single-zone thermal network, internal radiative gains are applied to the ceiling and external wall in an area-weighted manner while in the three-zone network, these gains are assumed to go to ceiling and floor equally just for simplicity. In this initial study, all zones that are coupled to these three zones are assumed to have a fixed temperature of 22˚C, which include all coupled zones in the 1st and 3rd floors as well as the stair space and lobby for the 2nd floor. As a result of this assumption, all adjacent walls (excluding adjacent floors and ceilings) that are exposed to the same air temperature can be lumped into one boundary wall for a specific zone. For example, zone 2 is adjacent to stair space and lobby through west and east walls respectively and these two adjacent walls are lumped as one wall subject to the same boundary condition. This lumping approach would reduce the size of the estimation problem below significantly.

4.2 TRNSYS Simulation Results

Figures 6 and 7 show TRNSYS simulation results for a three-day period (650th to 722nd hours of the year) for this building located at Philadelphia, PA. This period is used to present all testing results for the rest of this paper. Figure 6 shows zone-wise temperatures and ambient temperature and Figure 7 shows all energy inputs to the three zones. Cooling setpoints are 29 ℃ during unoccupied periods and 26 ℃ in the occupied period. Heating setpoints are 15 ℃ in the unoccupied period and 20 ℃ for occupancy. These simulation results are during the winter time so there is heating for all three zones. Zone 2 has a window facing east while zone 3 has a larger window facing west, so peaks of solar radiation are occurring during morning time for zone 2 and in the afternoon for zone 3. Zone 8 has windows and walls with all of the four orientations so the solar radiation has longer effects for zone 8 compared to the other two zones. But due to the larger external wall area, zone 8 has more coupling to ambient temperature so it needs more heating during occupied periods. Zone 3 has only heating for the presented interval, but it actually has cooling for some days even in the winter time because of solar radiation transmitted through the large window on the west wall. Zone 2 and zone 3 have only heating for the whole simulation period (first 1000 hours of the year).

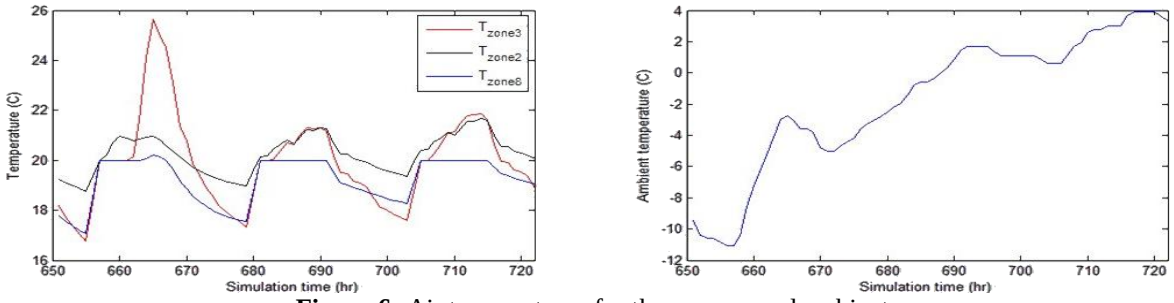

Figure 6: Air temperatures for three zones and ambient.

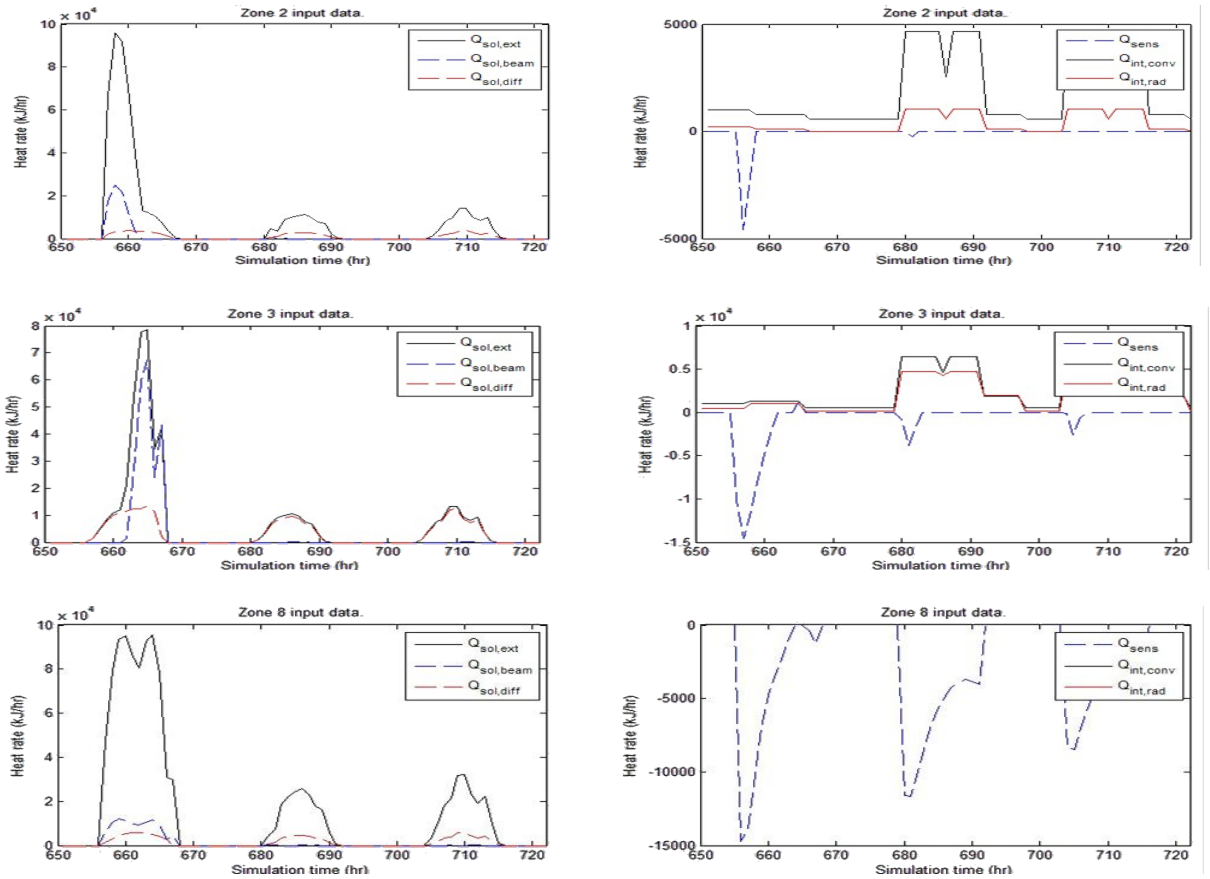

Figure 7: Solar radiation, internal heat gains and sensible heating or cooling of zones.

4.3 Zone-Wise Training

Applying the inverse modeling techniques described above, each zone model can be trained independently with the other two zone temperatures being boundary conditions. Results during the testing period are shown in Figure 8 for three zones. The predictions are reasonable but this training approach results in different zone-to-zone coupling parameters for each of the individual zone models which leads to an overall energy imbalance for the three zones considered together.

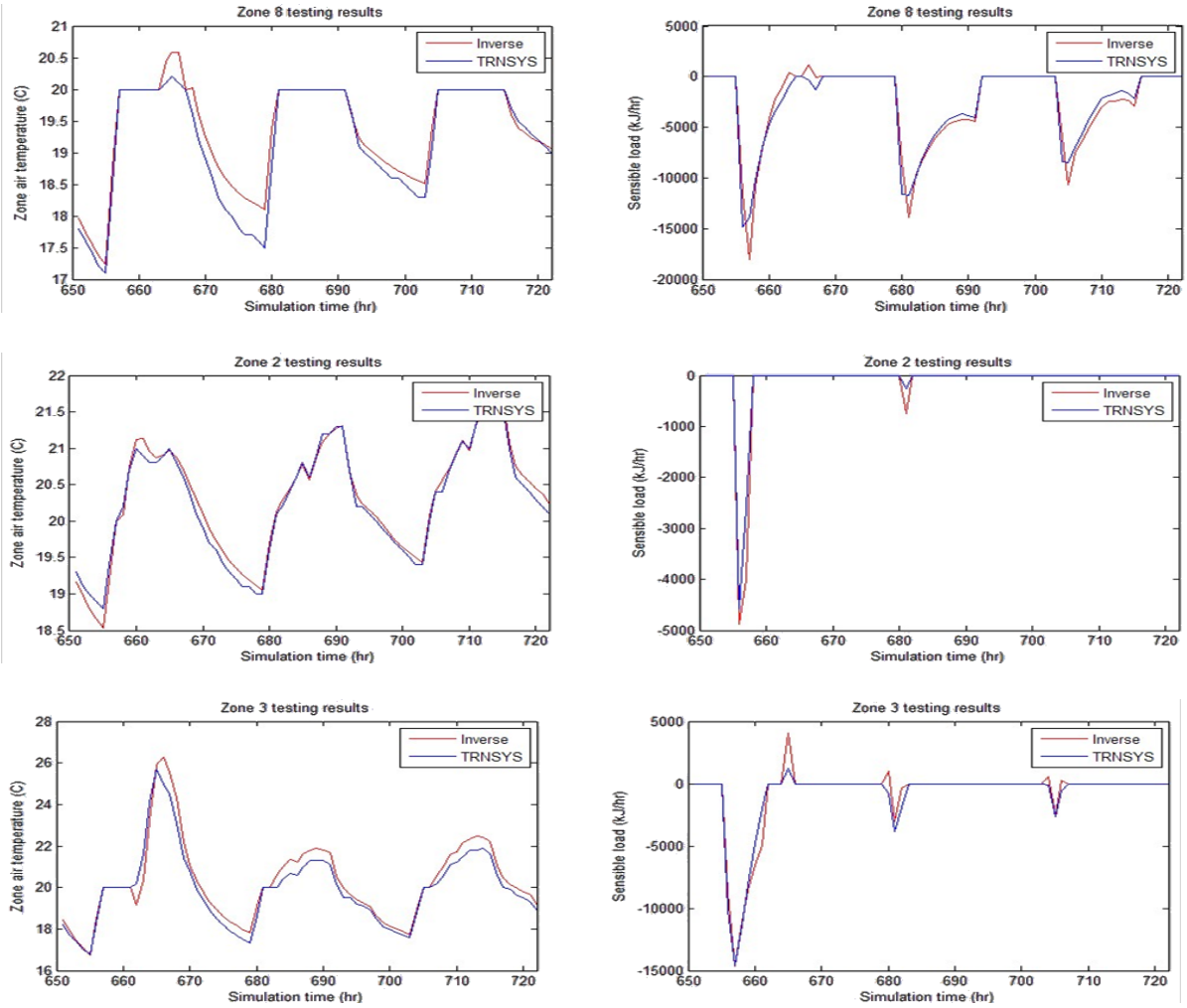

Figure 8: Zone air temperature predictions from zone-wise trained model and TRNSYS model.

4.4 Multi-Zone Coupled Training

In order to capture unique zone-to-zone coupling factors, a coupled multi-zone structure should be used and estimation should be performed for this coupled problem. Figure 5 shows a coupled thermal network for the three zones. In the coupled training process, all wall temperature nodes along with zone air nodes are combined into a single state vector. Each iteration of the training process requires the solution of a relatively large state-space model as compared with three separate solutions for three smaller problems with zone-wise training. This increases the computational requirements for each iteration. Also, the algorithm for parameter estimation is applied to a much larger dimensional search space (approximately three times larger for this case study) as compared with three separate smaller parameter estimation problems. The resultant estimation problem becomes very difficult to solve using the previously described solver.

Figure 9 shows performance of the model which was trained using 100 multi-start points. The errors are significantly larger than those for zone-wise training. This is undoubtedly because the parameter estimation procedure is determining a local minimum.

4.5 Multi-Zone Heuristic Training

The zone-wise training approach is not able to provide a single set of zone-to-zone coupling parameters but provides reasonable predictions and is computationally tractable. The multi-zone coupled training method determines unique coupling factors, but it leads to a large model structure and high-dimensional estimation problem, which is not easy to solve using the proposed training techniques. Therefore, a heuristic training scheme was investigated that combines elements of both training approaches.

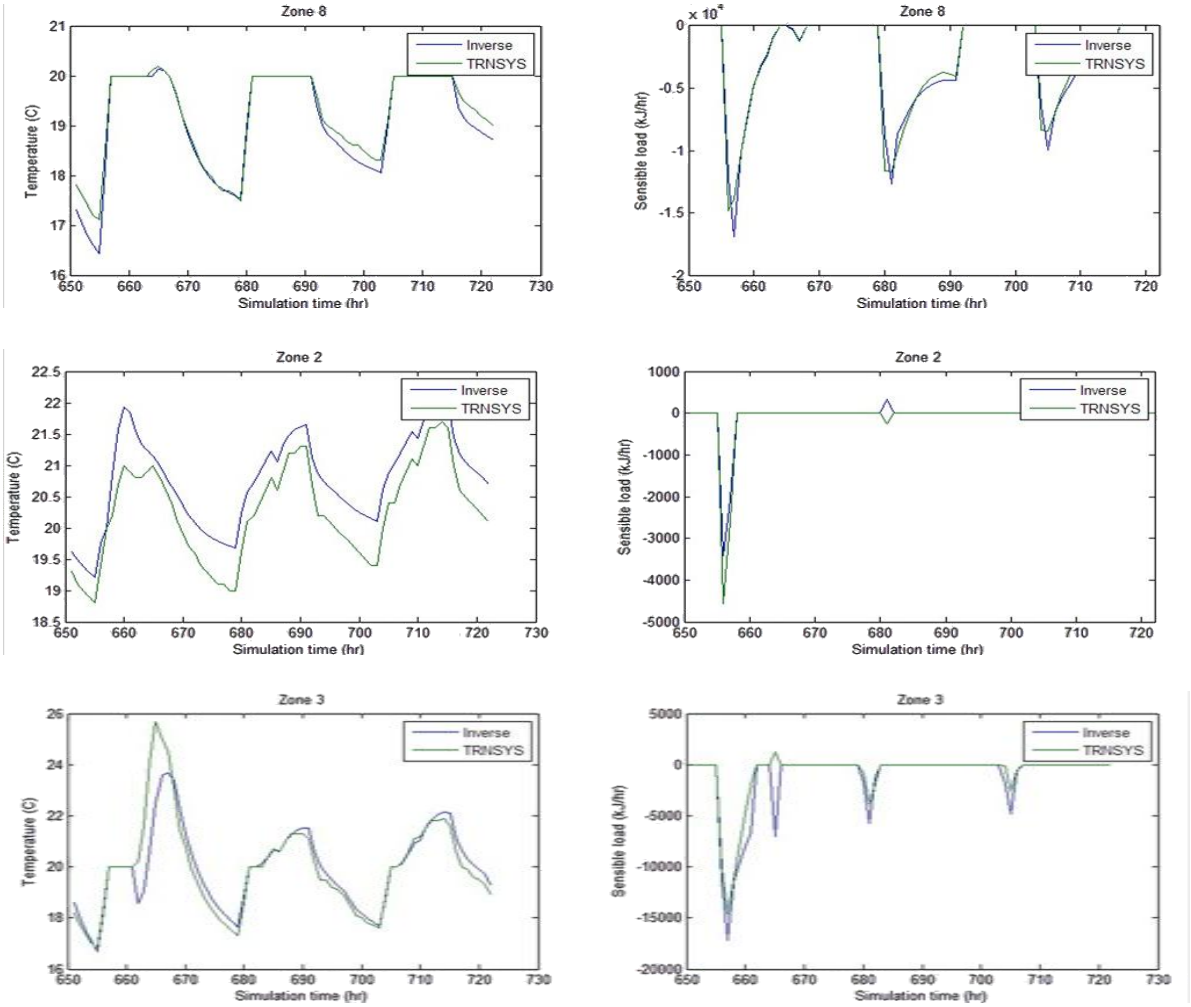

Figure 9: Multi-zone coupled training results.

If the inter-zonal heat transfer is relatively small compared to other heat transfer paths, then zone-wise training can lead to zone models that are close to the optimum except for the coupling parameters. This is the basis for the heuristic strategy depicted in Figure 10 for a two-zone case. First, the individual zone models are trained assuming fixed coupling factors based on initial guesses. The zone model parameters are then used as fixed values for training the coupling parameters. These estimated coupling parameter values are then plugged back into the lower level zone-wise training process to tune the non-coupling parameters. The iterative process continues until satisfactory results are reached. This approach reduces the computation requirements and improves final model results.

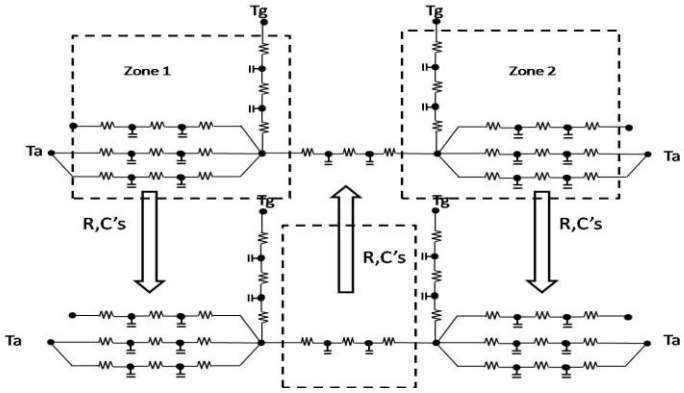

Figure 10: A two-zone heuristic training scheme illustration.

Figure 11 shows performance comparisons of the model predictions with TRNSYS results. Table 1 shows comparisons of RMSE errors associated with the training period for the three methods. The heuristic approach provides a single set of coupling factors. The overall accuracy is better than the coupled training approach and similar to the zone-wise training that utilizes separate coupling factors for each zone.

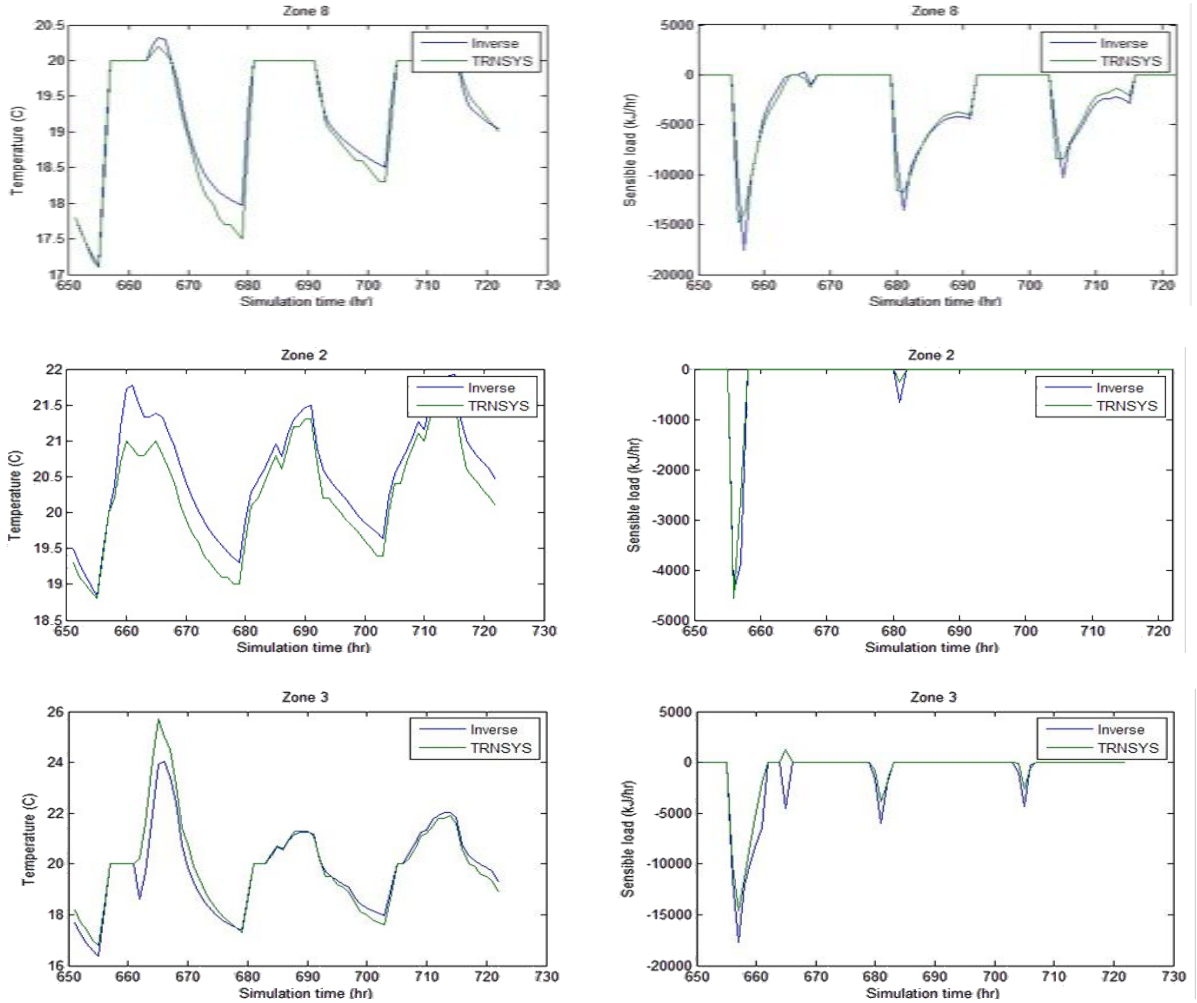

Figure 11: Multi-zone heuristic training results.

Table 1: Model performance (temperature prediction RMS error in ˚C and load prediction relative RMS error in %) comparison for different training processes.

		Zone 8	**Zone 2**	**Zone 3**
Zone-wise training	Temperature	0.23	0.174	0.51
	Load	4.42	2.03	4.28
Coupled training	Temperature	0.477	0.456	0.794
	Load	4.15	4.3	7.6
Heuristic training	Temperature	0.27	0.36	0.57
	Load	4.10	2.20	5.6

5. CONCLUSION

The inverse modeling techniques presented in this paper were implemented for a three-zone case study and the models obtained were able to provide reasonably accurate predictions. Zone-wise training can generate the most accurate model but it is not realistic, because it does not determine unique coupling factors for inter-zonal heat transfer. A coupled training approach involves determination of unique coupling factors but the dimensionality of

the parameter estimation problem makes it difficult to determine a global optimum solution. Therefore, a heuristic training process was developed that provides unique coupling factors in a computational efficient manner. The model obtained via this heuristic training process has performance almost as good as the model obtained using zone-wise training.

REFERENCE

1. Chaturvedi, N., 2000, "Analytical tools for dynamic building control", Masters Thesis, Herrick Laboratories, West Lafayette, Indiana.
2. Chaturvedi, N. and Braun, J.E., 2002, "An inverse gray-box model for transient building load prediction", *HVAC&R Research*, Vol. 8, No. 1, pp. 73-99.
3. Seem, J.E., S.A. Klein, W.A. Beckman, and J.W. Mitchell, 1989, "Transfer functions for efficient calculations of multi-dimensional heat transfer", *Journal of Heat Transfer-Transactions of the ASME* 111(1):5-12.
4. Aird, T.J. and Rice, J.R., 1977, "Systematic search in high dimensional sets", *SIAM Journal on Numerical Analysis*, Vol.14, pp. 296-312
5. K. Madsen, H.B. Nielsen and O. Tingleff, 2004, "Methods for nonlinear least squares problems", Informatics and Mathematical Modeling, Technical University of Denmark.
6. R. C. Aster, B. Borchers and C.H. Thurber, 2005, "Parameter estimation and inverse problems".
7. Arasteh, D., Kohler, C. and Griffith, B., 2009, "Modeling Windows in Energy Plus with Simple Performance Indices", Lawrence Berkeley National Laboratory.
8. Cai, J. and Braun, J.E., "An Efficient and Robust Training Methodology for Inverse Building Modeling", SimBuild 2012.
9. TRNSYS 17, 2010, Solar Energy Laboratory, University of Wisconsin-Madison.
10. EnergyPlus 7.0, 2011, http://apps1.eere.energy.gov/buildings/energyplus/, US Department of Energy.

ACKNOWLEDGEMENT

This work was supported by the Department of Energy through the Energy Efficient Buildings Hub.

NOMENCLATURE

$\dot{Q}_{sol,e}$ =rate of solar radiation incident on the lumped external walls

$\dot{Q}_{sol,c}$ = rate of solar radiation incident on the roof (ceiling)

$\dot{Q}_{sol,trans}$ = rate of solar radiation transmitted through windows to the inside

$\dot{Q}_{rad,c}$ = radiative internal gains per unit time transmitted to the ceiling

$\dot{Q}_{rad,e}$ = radiative internal gains per unit time transmitted to the external walls

$\dot{Q}_{conv}$ = convective internal gains per unit time

T	= temperature
R	= resistor
c	= capacitor
e	= external wall
i	= internal wall
c	= roof (ceiling)
g	= ground
z	= zone air
a	= ambient air
wi	= windows
mix	= mixed array of load and temperature in mixed training mode
bm	= benchmark data (training data)